Derivation and evaluation of Monte Carlo estimators of the scattering equation using the Ward BRDF and different sample allocation strategies

Carlos Lopez Garces[a,1], Nayeong Kong[b,1]

[a] *Department of Mathematics, Indiana University East, Richmond, IN 47374, USA*
[b] *Department of Mathematics, Indiana University East, Richmond, IN 47374, USA*

Abstract

We derive the analytic form of three of the Monte Carlo estimators of Sbert et al. [1] for the scattering equation, using the Ward BRDF and a cosine-weighted environment map. We also present a qualitative evaluation of each of the three estimators, which we implemented as extensions to the PBRT renderer [4]. The resulting rendered images are of varying convergence rates and variances that are consistent with the results obtained by Sbert et al. [1].

Keywords: Monte Carlo estimators, Scattering equation, Multiple Importance Sampling, Physically based rendering

1. Introduction

In Sbert et al. [1], the authors investigate the behavior of new balance heuristic estimators and new non-balance heuristic estimators for the scattering equation L_o used in physically-based rendering. The novelty of some of these estimators resided in the sample allocation strategy that they used, i.e. the way in which each of them assigns the sample count $N_i, i = 1, 2, ..., n$ to each of the sampling techniques employed.

The estimators and sample allocation strategies they evaluated are the balance heuristic with equal count of samples [3], a non-balance heuristic with sample count proportional to the variances of the sampling techniques, and a new heuristic where the ratio of sample count per sampling technique to the total count of samples is inversely proportional to the second moment of the distribution of each technique. They evaluated these estimators using a cosine-weighted environment map L_i and a Lafortune-Phong BRDF [8]. The results were given in terms of variance and variance times cost, which they used to give general conclusions about the performance of each estimator.

Email addresses: clopezga@iu.edu (Carlos Lopez Garces), kongna@iu.edu (Nayeong Kong)

Our goal is to apply their work and evaluate qualitatively the results of the same set of estimators and sample allocation strategies using a different pair of incident radiance function L_i and BRDF. This assessment involved the implementation of the aforementioned estimators and we used this implementation to render images that validated the results of Sbert et al. [1] extended to this pair of functions.

We begin by giving the reader a brief introduction to the important concepts behind Sbert et al. [1], presenting relevant results published previously. We then examine how Sbert et al. obtained their estimators and show we obtained ours using their methodology. At the end, we present our qualitative assessment.

2. Concepts and previous Work

2.1. Monte Carlo estimators (for definite integrals)

When a function $f : \Omega \to \mathbb{R}$ doesn't have a known closed form or its definite integral doesn't have analytic solutions, the value of $\int_\Omega f(x)dx$ can be estimated using a Monte Carlo estimator if the value of f can be sampled or evaluated at sample points drawn from some probability distribution. A Monte Carlo estimator is defined as follows.

Definition 1. *Let $(X_1, X_2, ..., X_N)$ be a random sample of a given distribution and f a function of interest. Then the Monte Carlo estimator of $\int_\Omega f(x)dx$ is given by*

$$F_N = \frac{1}{N} \sum_{i=1}^{N} \frac{f(X_i)}{p(X_i)} \tag{1}$$

where $p(x)$ is the pdf of the chosen distribution and N is the number of samples drawn from it and used to evaluate f. The expected value of this estimator is the value of $\int_\Omega f(x)dx$:

$$E[F_N] = \int_\Omega f(x)dx \tag{2}$$

a fact that follows from the Strong Law of Large Numbers.

A Monte Carlo estimator of this form has a severe drawback, though: a large number N of samples may be needed to reduce variance. Several techniques for reducing the variance of the estimator while keeping the number of samples low exist (Kahn et al. [2]), but one of them has seen wider adoption in rendering: **importance sampling**.

2.2. Importance sampling

Importance sampling is a **variance reduction technique** based on the observation that the Monte Carlo estimator converges with fewer samples if the samples are taken from a distribution with density $p(x)$ that is similar in shape to the integrand $f(x)$. If $p(x)$ has the same shape as $f(x)$, then $p(x)$ will be

large where $f(x)$ is large in value, and small where $f(x)$ is small in value. Thus, samples of $f(x)$ where $f(x)$ is large will be taken with higher probability.

If variance is to be reduced, then we must avoid insufficient sampling of f where its value is large. However, finding a distribution that matches the shape of f over the entire domain Ω is difficult; this is usually the case when the integrand is a product of functions, $f(x) = g(x)h(x)$ for example: a pdf that samples $g(x)$ with low variance might sample $h(x)$ poorly with high variance. Since a single distribution won't suffice, **multiple importance sampling** employs more than one.

2.3. Multiple importance sampling

For each region of the domain Ω where f might be large, multiple importance sampling (MIS) constructs a sampling distribution that approximates f well on that region. In the original MIS formulation by Veach et al. [3], each of the sampling distributions involved can use a different number N_i of samples. This estimator has the following form:

Definition 2. *Let n be the number of sampling distributions involved, $w_i(x)$ a weighting function associated with the ith distribution, and $f(x)$ the function being estimated (which doesn't have a closed form, but whose value can be sampled). Then the MIS estimator of $\int_\Omega f(x)dx$ is given by*

$$F = \sum_{i=1}^{n} \frac{1}{N_i} \sum_{j=1}^{N_i} \frac{f(X_{ij})w_i(X_{ij})}{p_i(X_{ij})} \tag{3}$$

where $p_i(x)$ is the pdf of the ith distribution.

Referring again to the example product $f(x) = g(x)h(x)$, an MIS estimator for $\int_\Omega f(x)dx$ could be

$$\frac{1}{N_g} \sum_{i=1}^{N_g} \frac{g(X_i)h(X_i)w_g(X_i)}{p_g(X_i)} + \frac{1}{N_h} \sum_{j=1}^{N_h} \frac{g(Y_j)h(Y_j)w_h(Y_j)}{p_h(Y_j)} \tag{4}$$

where X and Y are random variables distributed according to p_g and p_h, respectively, and $p_g(x) \propto g(x)$ and $p_h(y) \propto h(x)$.

The weighting function $w_i(x)$ eliminates large variance spikes caused by mismatches between the integrand f and the pdf p. It also keeps the estimator unbiased if it satisfies the following properties:

$$f(x) \neq 0 \Rightarrow \sum_{i=1}^{N} w_i(x) = 1 \tag{5}$$

$$p_i(x) = 0 \Rightarrow w_i(x) = 0 \tag{6}$$

A widely used weighting function is the so-called **balance heuristic** (Pharr et al. [4]):

Definition 3. *The balance heuristic is given by*

$$w_i(x) = \frac{N_i p_i(x)}{\sum_j N_j p_j(x)} \tag{7}$$

where the denominator is the sum of the pdfs of all the sampling distributions involved, weighted by their respective number of samples.

Since the first appearance of the balance heuristic in the literature (Veach et al. [3]), a few weighting functions have been proposed that yield substantially lower variance. Kondapaneni et al. [5], for instance, derived optimal weighting functions that minimize the variance of an MIS estimator, given a fixed set of sampling distributions.

Kondapaneni et al. [5] also declared that a *significant limitation* of MIS is its wasteful approach when a sensible **sample allocation** strategy isn't in place: sampling a given distribution i has its own unique cost and if the weighting function gives a near-zero weight to the N_i samples of that distribution, then their contribution is negligible and the sampling cost is thus incurred in vain.

2.4. Sample Allocation

Sample allocation refers to the action of setting the number of samples N_i that are drawn from each distribution i. In the original formulation of MIS, Veach et al. [3] argued that *"no strategy is much better than that of simply setting all [sample counts] equal"*, but that statement has been challenged since and proven to be wrong. The following are publications that set out to derive optimal sample allocation strategies:

Pajot et al. [6] developed the notion of *representativity* of a sampling distribution that measures the relevance of a sampling distribution for a given integrand. The representativity of each of the distributions in the chosen set is used to perform importance sampling on the sampling distributions themselves; a form of metaimportance sampling indeed. Sampling distributions with a higher degree of representativity for a given integrand are favored with a higher number of samples. Lu et al. [7] introduced a second-order approximation of variance for the balance heuristic and, based on this approximation, an automatic allocation of samples as well (for direct lighting only and without prior knowledge of the characteristics of the scene). Finally, Sbert et al. are perhaps the researchers that have advanced the problem area of sample allocation the most in recent years. Sbert et al. [10] showed that the optimal sample allocation must equalize the second moment of the weighted estimates corresponding to the individual sampling distributions; Sbert et al. [11] elaborated on prior results to design an approximate sample allocation solution; and Sbert et al. [1] introduced a new heuristic where the ratio of sample count per sampling technique to the total count of samples is inversely proportional to the second moment of the distribution of each technique and that is better than the balance heuristic with equal sample count per technique.

2.5. Scattering equation and BRDFs

The estimators studied and developed by Sbert et al. [1] are of the integral in the **scattering equation**.

Definition 4. *The scattering equation computes radiance L_o reflected by a surface at a point p in the direction ω_o. It is given by*

$$\begin{aligned} L_o(p,\omega_o) &= \int_{S^2} f(p,\omega_o,\omega_i) L_i(p,\omega_i) |\cos\theta_i| d\omega_i \\ &= \iint_{\theta,\phi} f(p,\omega_o,\omega_i) L_i(p,\omega_i) |\cos\theta_i| \sin\theta d\theta d\phi \\ &\approx \frac{1}{N} \sum_{j=1}^{N} \frac{f_r(p,\omega_o,\omega_j) L_i(p,\omega_j) |\cos\theta_j|}{p(\omega_j)} \end{aligned} \tag{8}$$

where f_r is the Bidirectional Reflectance Distribution Function, or BRDF, that describes how the surface reflects incident radiance L_i coming from direction ω_i. Solid angles ω_o and ω_i are typically expressed in spherical coordinates (θ, ϕ), where $\theta \in [0, \pi/2]$ is measured from the surface normal and $\phi \in [0, 2\pi]$.

We refer the reader to Pharr et al [4] for an in-depth exposition of these concepts.

The reader should now be acquainted with most of the relevant concepts. The following section examines more closely the procedure followed by Sbert et al. [1] to obtain the estimators of interest for a very particular case. We will then follow that procedure on our own choice of functions.

3. Estimators for the Lafortune-Phong BRDF and cosine-weighted hemisphere environment map

Sbert et al. [1] studied the estimators and sample allocation strategies of interest using the specular term of Lafortune-Phong BRDF f_r [8] and a cosine-weighted environment map as the source of incident radiance $L_i = R\cos\theta_i$. A description of this BRDF is warranted.

Definition 5. *The specular term of the Lafortune-Phong BRDF is given by*

$$f_r(\omega_o,\omega_i) = \rho_s \frac{m+2}{2\pi} \cos^m \theta_i \tag{9}$$

where ρ_s is the specular reflectivity, i.e. the fraction of the perpendicularly incoming radiance that is reflected specularly, and m controls the sharpness of specular reflections.

To exemplify the work we'll do, we present first the estimators for the pair of functions chosen by Sbert et al. [1]; we then present our own. The integral of interest is

$$
\begin{aligned}
L_o(p,\omega_o) &= \iint_{\theta_i,\phi} \left(\rho_s \frac{m+2}{2\pi}\cos^m\theta_i\right)(R\cos\theta_i)\,|\cos\theta_i|\sin\theta_i d\theta_i d\phi \\
&= 2\pi R\int_{\theta_i=0}^{\pi/2}\left(\rho_s \frac{m+2}{2\pi}\cos^m\theta_i\right)\cos^2\theta_i\sin\theta_i d\theta_i \\
&= 2\pi R\int_{x=0}^{1}\left(\rho_s \frac{m+2}{2\pi}x^{m+1}\right)x dx \\
&= 2\pi R\int_{x=0}^{1} g_1(x)g_2(x)dx
\end{aligned}
\tag{10}
$$

where the substitution $x = cos\theta_i$ was made so that $x \in [0,1]$, like a uniform random variable. Observe that $g_1(x)$ traces back to $f_r(\omega_o,\omega_i)$ times a factor of x and that $g_2(x) = x$.

Following the MIS principle, we sample $g_1(x)$ and $g_2(x)$ using probability density functions whose shapes approximate those of the functions in question. According to Lafortune et al. [8], the following pdf can be used to sample the specular term of the BRDF

$$
p_1(x) = \frac{m+1}{2\pi}\cos^m x \tag{11}
$$

which samples according to the $\cos^m\theta_i$ factor so that the direction is chosen inside the specular lobe. For $g_2(x) = x = \cos\theta$, Pharr et al. [4] give the following density function

$$
p_2(\omega) = \frac{4cos\theta}{\pi} \tag{12}
$$

which corresponds to a cosine-weighted distribution.

Having factorized the integrand and found probability density functions that approximate the shape of the factors, the Monte Carlo estimator with equal count of samples N with balance heuristic (Veach et al. [3]) is given by

$$
\hat{F}_{eq} = 2\pi R\sum_{i=1}^{n}\sum_{j=1}^{N_i}\frac{g_1(X_{ij})g_2(X_{ij})}{\sum_{k=1}^{n}N_k p_k(X_{ij})} = 2\pi R\sum_{i=1}^{2}\sum_{j=1}^{N_i}\frac{\left(\rho_s\frac{m+2}{2\pi}X_{ij}^{m+1}\right)X_{ij}}{Np_1(X_{1j}) + Np_2(X_{2j})} \tag{13}
$$

This estimator assigns the same number of samples to each of the sampling strategies and weighs their contribution using the balance heuristic of Definition 3.

Next, the non-balance heuristic with sample count proportional to the variances of the sampling techniques of Sbert et al. [1] represents an improvement in terms of variance over the equal counts balance heuristic estimator. Here the number of samples assigned to each sampling strategy i is proportional to the variance $\sigma^2_{i,eq}$ of the equal counts balance heuristic estimator that uses the corresponding sampling strategy, that is, $N_i \propto \sigma^2_{i,eq}$:

$$\hat{F}_{\sigma^2} = \frac{R}{N_1}\sum_{j=1}^{N_1}\frac{\left(\rho_s\frac{m+2}{\pi}X_{1j}^{m+1}\right)X_{1j}}{p_1(X_{1j})+p_2(X_{2j})} + \frac{R}{N_2}\sum_{j=1}^{N_2}\frac{\left(\rho_s\frac{m+2}{\pi}X_{2j}^{m+1}\right)X_{2j}}{p_1(X_{1j})+p_2(X_{2j})} \tag{14}$$

with $\sigma^2_{i,eq} = Var(\hat{F}_{eq,i})$.

Finally, Sbert et al. [1] present another estimator with $\frac{N_i}{N} \propto \frac{1}{m_i^2}$ where m_i^2 is the second moment of sampling distribution i. The expression for the estimator is the same as in Equation 14.

4. Estimators for the Isotropic Ward BRDF and cosine-weighted hemisphere environment map

Montes and Ureña [9] classified the BRDFs they studied as empirical, theoretical, and experimental. Experimental BRDFs are obtained using a gonioreflectometer, a device that mechanically varies a light source illuminating a surface and that measures the ratio of radiance reflected from the surface to the incident radiance. One such BRDF is our choice of study: the Ward BRDF in its isotropic form.

With microfacets at the core of the model, the BRDF that Ward [12] formulated has a diffuse component and an anisotropic lobe modeled by an elliptic Gaussian and controlled by a small set of parameters: ρ_s is the specular reflectance, and α_x and α_y are the standard deviations of the microfacet slopes in the x and y directions, respectively. When $\alpha_x = \alpha_y$, the model specializes to the isotropic case, which is our particular subject of study, given that it's simpler than the more general anisotropic version.

Definition 6. *The isotropic Ward BRDF is given by*

$$f_r^{iso}(\theta_o,\phi_o,\theta_i,\phi_i) = \frac{\rho_d}{\pi} + \frac{\rho_s}{4\pi\alpha^2\sqrt{\cos\theta_i\cos\theta_o}}e^{-\frac{\tan^2\theta_h}{\alpha^2}} \tag{15}$$

where ρ_d in the diffuse term is the diffuse reflectance of the surface, α is the standard deviation of the slope of microfacets, and θ_h is measured from the normal of the surface and corresponds to the halfway vector between the reflection and incidence vectors, $\mathbf{o}$ *and* $\mathbf{i}$*, assuming that they lie on the same plane as* $\mathbf{n}$ *and that they are unit vectors:*

$$\mathbf{h} = \frac{\mathbf{i}+\mathbf{o}}{\|\mathbf{i}+\mathbf{o}\|} \tag{16}$$

so that $\theta_h = \left|\frac{\theta_i-\theta_o}{2}\right|$ *and*

$$
\begin{aligned}
\tan^2\theta_h &= \tan^2\left|\frac{\theta_i}{2}-\frac{\theta_o}{2}\right| \\
&= \left(\frac{\sin\left|\frac{\theta_i}{2}-\frac{\theta_o}{2}\right|}{\cos\left|\frac{\theta_i}{2}-\frac{\theta_o}{2}\right|}\right)^2 \\
&= \left(\frac{\sin\frac{\theta_i}{2}\cos\frac{\theta_o}{2}-\cos\frac{\theta_i}{2}\sin\frac{\theta_o}{2}}{\cos\frac{\theta_i}{2}\cos\frac{\theta_o}{2}+\sin\frac{\theta_i}{2}\sin\frac{\theta_o}{2}}\right)^2 \\
&= \left(\frac{\sqrt{\frac{1-\cos\theta_i}{2}}\cos\frac{\theta_o}{2}-\sqrt{\frac{1+\cos\theta_i}{2}}\sin\frac{\theta_o}{2}}{\sqrt{\frac{1+\cos\theta_i}{2}}\cos\frac{\theta_o}{2}+\sqrt{\frac{1-\cos\theta_i}{2}}\sin\frac{\theta_o}{2}}\right)^2
\end{aligned}
\tag{17}
$$

after the application of well-known trigonometric identities.

The reader familiar with microfacet models will notice the absence of explicit Fresnel coefficients and geometrical attenuation factors. Ward [12] explains that these factors are encapsulated in the normalization factor $\frac{1}{4\pi\alpha^2}$, so long as α is not much greater than 0.2.

As before, the integral of interest is the scattering equation of Definition 4. To obtain its Monte Carlo estimators, we first turn it into an integral over the interval $[0,1]$ with the integrand being a product of two functions:

$$
\begin{aligned}
&L_o(p,\theta_o,\phi_o) \\
&= \int_0^{\pi/2}\int_0^{2\pi} (f_r^{iso}(p,\theta_o,\phi_o,\theta_i,\phi_i)L_i(p,\theta_i,\phi_i)|\cos\theta_i|)\sin\theta_i d\phi_i d\theta_i \\
&= 2\pi\int_0^{\pi/2}\left(\frac{\rho_d}{\pi}+\frac{\rho_s}{4\pi\alpha^2\sqrt{\cos\theta_i\cos\theta_o}}e^{-\frac{\tan^2\left|\frac{\theta_i}{2}-\frac{\theta_o}{2}\right|}{\alpha^2}}\right)(R\cos\theta_i)\cdot|\cos\theta_i|\cdot\sin\theta_i d\theta_i \\
&= 2\pi\int_0^{\pi/2}\left(\frac{\rho_d}{\pi}+\frac{\rho_s e^{-\frac{\left(\frac{\sqrt{\frac{1-\cos\theta_i}{2}}\cos\frac{\theta_o}{2}-\sqrt{\frac{1+\cos\theta_i}{2}}\sin\frac{\theta_o}{2}}{\sqrt{\frac{1+\cos\theta_i}{2}}\cos\frac{\theta_o}{2}+\sqrt{\frac{1-\cos\theta_i}{2}}\sin\frac{\theta_o}{2}}\right)^2}{\alpha^2}}}{4\pi\alpha^2\sqrt{\cos\theta_i\cos\theta_o}}\right)(R\cos\theta_i)\cdot|\cos\theta_i|\cdot\sin\theta_i d\theta_i
\end{aligned}
\tag{18}
$$

Now let $x=\cos\theta_i$. Then $\frac{dx}{d\theta_i}=-\sin\theta_i$, and

$$
\begin{aligned}
&L_o(p,\theta_o,\phi_o) \\
&= 2\pi \int_0^1 \left(\frac{\rho_d}{\pi} + \frac{\rho_s e^{-\frac{\left(\frac{\sqrt{\frac{1-x}{2}}\cos\frac{\theta_o}{2} - \sqrt{\frac{1+x}{2}}\sin\frac{\theta_o}{2}}{\sqrt{\frac{1+x}{2}}\cos\frac{\theta_o}{2} + \sqrt{\frac{1-x}{2}}\sin\frac{\theta_o}{2}}\right)^2}{\alpha^2}}{4\pi\alpha^2\sqrt{x\cos\theta_o}} \right) (Rx)\cdot|x|dx \\
&= \frac{2}{3}\rho_d R + 2\pi R \int_0^1 \left(\frac{\rho_s e^{-\frac{\left(\frac{\sqrt{\frac{1-x}{2}}\cos\frac{\theta_o}{2} - \sqrt{\frac{1+x}{2}}\sin\frac{\theta_o}{2}}{\sqrt{\frac{1+x}{2}}\cos\frac{\theta_o}{2} + \sqrt{\frac{1-x}{2}}\sin\frac{\theta_o}{2}}\right)^2}{\alpha^2}}{4\pi\alpha^2\sqrt{x\cos\theta_o}} x \right) x dx \\
&= \frac{2}{3}\rho_d R + 2\pi R \int_0^1 g_1(x) g_2(x) dx.
\end{aligned}
\tag{19}
$$

Following the MIS principle, we sample $g_1(x)$ and $g_2(x)$ using probability density functions whose shapes approximate those of the functions in question. In the case of $g_1(x)$, we derive a pdf for the specular term out of the one formulated by Walter [13]:

$$
p_{1,s}(\mathbf{i}) = \frac{1}{4\pi\alpha^2(\mathbf{h}\cdot\mathbf{o})\cos^3\theta_h} e^{-\frac{\tan^2\theta_h}{\alpha^2}} \tag{20}
$$

Assuming that $\mathbf{h}$ and $\mathbf{i}$ are unit vectors and letting $\theta_{oh} = \frac{\theta_o+\theta_i}{2}$ be the angle between them, we make the following substitutions in $p_{1,s}$:

$$
\begin{aligned}
\mathbf{h}\cdot\mathbf{o} &= \cos\frac{\theta_o+\theta_i}{2} \\
&= \cos\frac{\theta_i}{2}\cos\frac{\theta_o}{2} - \sin\frac{\theta_i}{2}\sin\frac{\theta_o}{2} \\
&= \sqrt{\frac{1+\cos\theta_i}{2}}\cos\frac{\theta_o}{2} - \sin\sqrt{\frac{1-\cos\theta_i}{2}}\sin\frac{\theta_o}{2} \\
&= \sqrt{\frac{1+x}{2}}\cos\frac{\theta_o}{2} - \sin\sqrt{\frac{1-x}{2}}\sin\frac{\theta_o}{2}
\end{aligned}
\tag{21}
$$

and

$$
\begin{aligned}
\cos^3\theta_h = \cos^3\left|\frac{\theta_i-\theta_o}{2}\right| &= \cos^3\frac{\theta_i-\theta_o}{2} \\
&= \left(\cos\frac{\theta_i}{2}\cos\frac{\theta_o}{2}+\sin\frac{\theta_i}{2}\sin\frac{\theta_o}{2}\right)^3 \\
&= \left(\sqrt{\frac{1+\cos\theta_i}{2}}\cos\frac{\theta_o}{2}+\sqrt{\frac{1-\cos\theta_i}{2}}\sin\frac{\theta_o}{2}\right)^3 \\
&= \left(\sqrt{\frac{1+x}{2}}\cos\frac{\theta_o}{2}+\sqrt{\frac{1-x}{2}}\sin\frac{\theta_o}{2}\right)^3
\end{aligned}
\tag{22}
$$

so that $p_{1,s}$ is given in terms of x by the following theorem:

Theorem 1. *The specular term of $g_1(x)$ can be sampled using the following pdf*

$$
p_{1,s}(x) = \frac{e^{-\frac{\left(\sqrt{\frac{1-\cos\theta_i}{2}}\cos\frac{\theta_o}{2}-\sqrt{\frac{1+\cos\theta_i}{2}}\sin\frac{\theta_o}{2}\right)^2}{\alpha^2}}}{4\pi\alpha^2\left(\sqrt{\frac{1+x}{2}}\cos\frac{\theta_o}{2}-\sin\sqrt{\frac{1-x}{2}}\sin\frac{\theta_o}{2}\right)\left(\sqrt{\frac{1+x}{2}}\cos\frac{\theta_o}{2}+\sqrt{\frac{1-x}{2}}\sin\frac{\theta_o}{2}\right)^3}
\tag{23}
$$

which has roughly the same shape as $g_1(x)$.

As for $g_2(x)$, it is the same as in Lafortune-Phong's, so we use the same density function of Equation 12.

With the $g_1(x)$ and $g_2(x)$ and their respective density functions defined in terms of $x = \cos\theta_i$, we may sample the value of x using a uniform random variable X and define in terms of it the Monte Carlo estimators that we wish to evaluate. Starting with the equal-count-of-samples estimator with balance heuristic:

Definition 7. *The equal count of samples Monte Carlo estimator with balance heuristic for the scattering equation when the BRDF is the Ward BRDF is given by*

$$
\begin{aligned}
\hat{F}_{eq} &= 2\pi R\sum_{i=1}^{2}\sum_{j=1}^{N}\frac{g_1(X_{ij})g_2(X_{ij})}{Np_1(X_{1j})+Np_2(X_{2j})} \\
&= 2\pi R\sum_{i=1}^{2}\sum_{j=1}^{N}\frac{\rho_s e^{-\frac{\varphi_{ij}^2}{\alpha^2}}X_{ij}^2}{N\frac{e^{-\left(\sqrt{\frac{1+X_{ij}}{2}}\cos\frac{\theta_o}{2}+\sqrt{\frac{1-X_{ij}}{2}}\sin\frac{\theta_o}{2}\right)^{-3}\frac{\varphi_{ij}^2}{\alpha^2}}}{4\pi\alpha^2\left(\sqrt{\frac{1+X_{ij}}{2}}\cos\frac{\theta_o}{2}-\sin\sqrt{\frac{1-X_{ij}}{2}}\sin\frac{\theta_o}{2}\right)}+N\frac{4X_{ij}^2}{\pi}}
\end{aligned}
\tag{24}
$$

where

$$
\varphi_{ij} = \frac{\sqrt{\frac{1-X_{ij}}{2}}\cos\frac{\theta_o}{2}-\sqrt{\frac{1+X_{ij}}{2}}\sin\frac{\theta_o}{2}}{\sqrt{\frac{1+X_{ij}}{2}}\cos\frac{\theta_o}{2}+\sqrt{\frac{1-X_{ij}}{2}}\sin\frac{\theta_o}{2}}
\tag{25}
$$

We now turn our attention to the non-balance heuristic estimator of Sbert et al. [1]. As discussed in the previous section, the sample allocation strategy implemented by this estimator assigns to each sampling technique a count of samples that is proportional to the variance of the equal-count-of-samples estimator that corresponds to that technique, that is, $N_i \propto \sigma^2_{i,eq}$. As such, the estimator for our Ward BRDF version has the same form as our estimator of Definition 7, except for the sample counts N_i found in the densities.

Definition 8. *The non-balance heuristic Monte Carlo estimator for the scattering equation when the BRDF is the Ward BRDF is given by*

$$\begin{aligned}\hat{F}_{eq} &= 2\pi R \sum_{i=1}^{2} \sum_{j=1}^{N} \frac{g_1(X_{ij}) g_2(X_{ij})}{N p_1(X_{1j}) + N p_2(X_{2j})} \\ &= 2\pi R \sum_{i=1}^{2} \sum_{j=1}^{N} \frac{\rho_s e^{-\frac{\varphi_{ij}^2}{\alpha^2}} X_{ij}^2}{N_i \frac{e^{-\left(\sqrt{\frac{1+X_{ij}}{2}} \cos\frac{\theta_o}{2} + \sqrt{\frac{1-X_{ij}}{2}} \sin\frac{\theta_o}{2}\right)^{-3} \frac{\varphi_{ij}^2}{\alpha^2}}}{4\pi\alpha^2 \left(\sqrt{\frac{1+X_{ij}}{2}} \cos\frac{\theta_o}{2} - \sin\sqrt{\frac{1-X_{ij}}{2}} \sin\frac{\theta_o}{2}\right)} + N_i \frac{4X_{ij}^2}{\pi}}\end{aligned} \tag{26}$$

where $N_i \propto \sigma^2_{i,eq}$, $\sigma^2_{i,eq} = Var(\hat{F}_{eq,i})$, and φ_{ij} is as in Definition 7.

Due to how complex the expression for $\hat{F}_{eq}$ is, we don't present one for $Var(\hat{F}_{eq})$. Instead, we use a numerical solution and compute it at run-time in the simulation presented in the next section.

Finally, the estimator presented by Sbert et al. [1] with balance heuristic weighting function and $\frac{N_i}{N} \propto \frac{1}{m_i^2}$ where m_i^2 is the second moment of sampling distribution i:

Definition 9. *The balance heuristic Monte Carlo estimator with $\frac{N_i}{N} \propto \frac{1}{m_i^2}$ for the scattering equation when the BRDF is the Ward BRDF has the same form as the estimator of Definition 8.*

In the following section, we describe an implementation of the Ward BRDF and the estimators of Definitions 7, 8, and 9 in PBRT, the renderer of Pharr et al. [4]. We also present qualitative results that compare rendered images produced with each of the 3 estimators.

5. Implementation and results

With the intention of evaluating qualitatively the relative rate of convergence of the three estimators, we implemented each of them in PBRT, the renderer of Pharr et al. [4]. While our original intention had been to write a simulation in the R language where we would compare the estimated value of L_o against the result of other forms of numerical approximations of the integral, the complexity of the Ward BRDF prevented us from doing that.

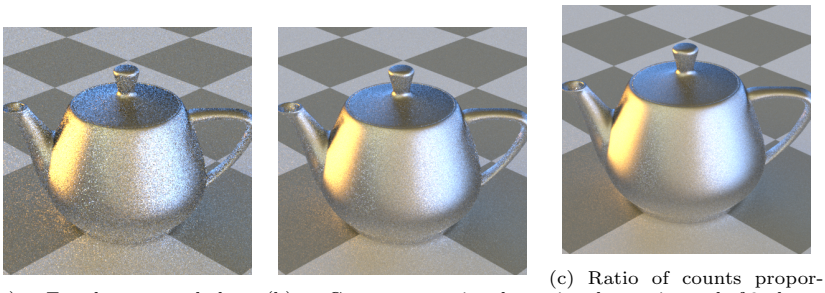

(a) Equal-counts balance heuristic

(b) Count-proportional-to-variance

(c) Ratio of counts proportional to reciprocal of 2nd moment

Figure 1: Comparison of images rendered by the 3 estimators

Along with the estimators, of course, we implemented the Ward BRDF (as a subclass of PBRT's BxDF class and implemented the required interface). The other implementation details of the simulation, such as the type of sampler and the type of integrator, were chosen somewhat arbitrarily: we employed a stratified sampler and a bidirectional path integrator; while we can't deny that these choices must have influenced the results, we decided to report our evaluation of the three estimators with these implementation details fixed. To compute the estimates of $Var(\hat{F}_{eq})$ and $\frac{1}{m_i^2}$, we leveraged the framework found in the supplemental code of Grittmann et al. [14], making changes as appropriate.

Figure 1 shows the classic Utah teapot with its material described by our implementation of the isotropic Ward BRDF and rendered using each of the three estimators with the same total number of samples. The noisier the image looks, the larger the variance is of the estimate of L of each pixel, that is, the estimate of the radiance that enters the camera through each pixel. The reader should be able to appreciate the increasing visual quality: the estimator of Definition 7 produces the noisiest image, while the estimator of Definition 9 produces the sharpest one, with the one that corresponds to Definition 8 lying somewhere in between.

Figure 2 shows the scene used by Veach et al. [3] in their demonstration of MIS. The original scene uses bars of increasing glossiness, but ours uses the same material on all the bars, a material described primarily by our isotropic Ward BRDF. The scene was designed to show the effects of MIS with varying configurations of light emission intensity, light source size, and material glossiness. We gave a much narrower purpose to the scene, though, and present here images of it that emphasize much more the differences in variance and convergence among our three estimators.

These qualitative results do not contradict the conclusions of Sbert et al. [1].

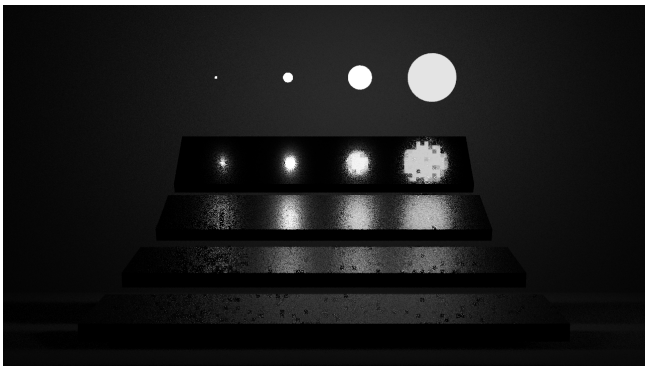

(a) Equal-counts balance heuristic

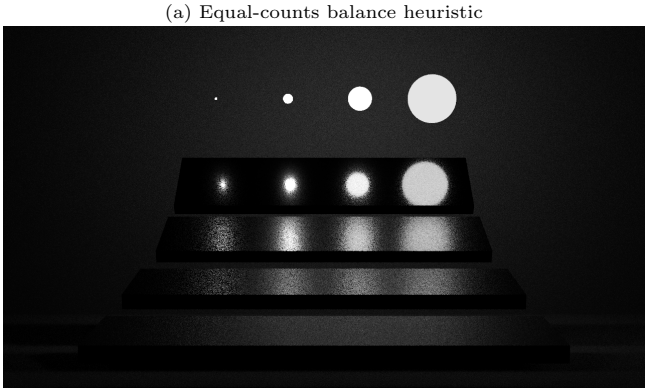

(b) Count-proportional-to-variance

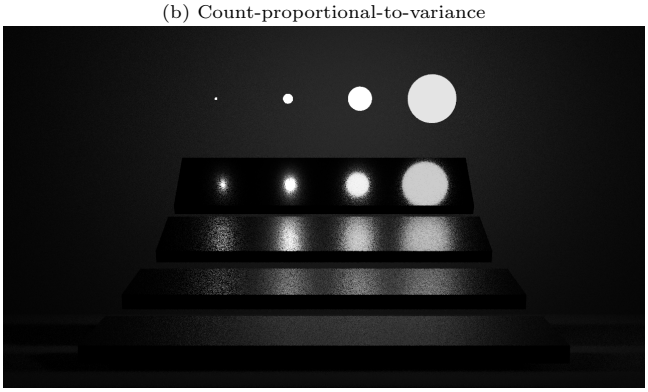

(c) Ratio of counts proportional to reciprocal of 2nd moment; Veach's test for MIS

Figure 2: Comparison of images rendered by the 3 estimators

6. Conclusion

In this paper, we studied three of the estimators examined by Sbert et al. [1], as well as the procedure they followed to obtain them for the scattering equation, the Lafortune-Phong BRDF, and a cosine-weighted environment map. We replicated that procedure to obtain estimators for the same equation, but with the Ward BRDF and a cosine-weighted environment map. Our simulation of these estimators produced rendered images of varying variance and convergence rates that are consistent with the results obtained by Sbert et al. [1].

7. Future Plan

We plan to extend our study to several other BRDF and incident radiance function pairs, while also generalizing some of the assumptions we made here.

References

[1] Mateu Sbert, Vlastimil Havran, and Laszlo Szirmay-Kalos, "Multiple importance sampling revisited: breaking the bounds" in EURASIP Journal on Advances in Signal Processing 2018

[2] Herman Kahn and A. W. Marshall, "Methods of Reducing Sample Size in Monte Carlo Computations" in Journal of the Operations Research Society of America 1953

[3] Eric Veach and Leonidas J. Guibas, "Optimally Combining Sampling Techniques for Monte Carlo Rendering" 1995

[4] Matt Pharr, Wenzel Jakob, and Greg Humphreys "Physically Based Rendering" 2016

[5] Ivo Kondapaneni et al., "Optimal Multiple Importance Sampling" 2019

[6] Anthony Pajot, Loic Barthe, Mathias Paulin, and Pierre Poulin, "Representativity for robust and adaptive multiple importance sampling" 2011

[7] Heqi Lu, Romain Pacanowski, and Xavier Granier, "Second-Order Approximation for Variance Reduction in Multiple Importance Sampling" in Computer Graphics forum, Volue 32, Issue 7; 2013

[8] Eric P. Lafortune and Yves D. Willems, "Using the Modified Phong Reflectance Model for Physically Based Rendering" 1994

[9] Rosana Montes and Carlos Ureña, "An Overview of BRDF Models" 2012

[10] Vlastimil Havran and Mateu Sbert, "Optimal Combination of Techniques in Multiple Importance Sampling" in Proceedings of the 13th ACM SIGGRAPH International Conference on Virtual-Reality Continuum and Its Applications in Industry, 2016

[11] Mateu Sbert and Vlastimil Havran, "Adaptive multiple importance sampling for general functions" in Vis Comput 33, 845–855 2017

[12] Gregory J. Ward, "Measuring and Modeling Anisotropic Reflection" in SIGGRAPH '92; 1992

[13] Bruce Walter, "Notes on the Ward BRDF" in Technical Report PCG-05-06; 2005

[14] Pascal Grittmann, Iliyan Georgiev, Philipp Slusallek, and Jaroslav Křivánek, "Variance-aware multiple importance sampling" in SIGGRAPH Asia '19; 2019